A new interferogram simulator : 2SIR. Study of coherence losses for tortured reliefs.

D. PETIT[(1)], F. ADRAGNA[(2)].

[(1)] Institut de Recherche en Informatique de Toulouse (IRIT)
TCI, Université Paul Sabatier, 118 route de Narbonne 31062 Toulouse Cedex, France
Ph: +33 5 61 55 63 20 Fax: +33 5 61 55 62 58 email: petit@irit.fr

[(2)] Centre National d'Etudes Spatiales (CNES)
QTIS/SR, 18 Avenue Edouard Belin, Bpi 811 31401 Toulouse France
email: frederic.adragna@cnes.fr

ABSTRACT

Recent developments in interferometric radar technique largely highlighted potentialities of radar interferometry for the generation of high resolution DEM (Digital Elevation Models). Nevertheless, the performances of this almost automatic process are strongly degraded for tortured reliefs and for vegetation areas. A research in progress with the CNES (Centre National d'Etudes Spatiales), CSSI (Communication & System, group "Systeme d'Information") and the IRIT (Institut de Recherche en Informatique de Toulouse) proposes to approach these phenomena by the means of simulation. So a new simulator, called 2SIR (Simulateur d'Images Radar & Simulateur d'Interférogrammes Radar), has been developed in which complex scenes can be described. As a first application, this simulator is used to reproduce and study coherence losses for tortured reliefs and the appropriateness of classical coherence to characterize interferograms quality is also discussed.

INTRODUCTION

SAR interferometric techniques have been already used for several years for the generation of Digital Elevation Model (DEM) [9][10][…]. Whereas processes are well known for ground with small slopes and for homogeneous or sporadic vegetation; on the other hand, in urban areas, or in any situations with involved interactions, these procedures are not adapted or accurate. In spite of its limitations, simulation is a very practical tool to approach complex cases, since ground measurements are not always available or easy to exploit.

Many simulators already make it possible to generate interferometric radar images, starting from DEM [8][11]; however, those are generally not adapted to the context of the high resolution in urban areas, or in vegetal domains, but are to the characteristics of bare soils. Indeed, it is often difficult to take into account the dielectric specificities of each surface element, to modelize vertical planes or overhang, and especially to simulate volumic interactions.

Therefore, the feature of the new simulator called 2SIR (Simulateur d'Images Radar & Simulateur d'Interférogrammes Radar) is to overcome the deficiencies of DEM by allowing complex situations to be described with the help of simple models. In this aim, it exploits 3 data bases which contain the "3D" information and the dielectric properties of the scene, and it can produce 4 types of images (see Fig 4). As its purpose is to simulate a realistic interferogram, it has been first tested on tortured reliefs to verify its capacity to reproduce coherence losses.

TECHNICAL FEATURES OF THE SIMULATOR

Data Bases

The Materials Data Base

In this data base, each type of material is characterized by 8 parameters for each type of polarization. The 3 parameters ρ_s, κ, ρ_0 quantify the backscattering coefficient σ (1), which has two components (2):

- A specular part, characterized by ρ_s, which specifies the specular contribution when then local angle of incidence θ' is null (Fig 3). The coefficient κ is a roughness parameter that reduces the width of the specular part.

- A scattering component characterized by ρ_0.

$$\sigma = 10\log(\rho) \quad (1)$$

$$\rho = \rho_s \exp(-\sin(\theta')/\kappa) + \rho_0 \cos(\theta') \quad (2)$$

These three parameters are computed by fitting data extracted from the Handbook of F. T. Ulaby and M. C.

Dobson [1]. An example of such a modelization is given in Fig. 1.

A fourth parameter defines the density of targets that will be randomly distributed on a surface or in a volume and a fifth one characterizes the vanishing coefficient for volumic interactions. Additional Red, Green and Blue parameters allow color of the material to be defined in the optical representation (merely to get a better representation rather than to simulate the material response in the optical domain)

An Objects Data Base

In order to describe the scene more easily, a few basic objects are provided. Examples are given in Fig. 2. The circles represent randomly distributed targets, which means that speckle would be modelized by a well-known Rayleigh distribution [2].

A Terrain Object Models Data Base

The scene is described in a Terrain Object Models Data Base (TOMDB ⊃ DEM), by basic objects defined in the Object Data Base (ODB) with some properties specified in the Materials Data Base (MDB). Each element of the TOMDB consists also in 2 links with the 2 other Databases, and an object descriptor that specifies the localization and the sizes of the object.

Images Generator

The images are computed in 2 steps (Fig. 3). First of all, targets are randomly distributed within objects, then returned echoes are added to simulate the radar response in an intermediate angular image. The aim of this preprocessing is to manage masked echoes (with the technique called z-buffering) and transparency, effects which can't be ignored with tortured reliefs. The second step consists of a summation of echoes registered at the same range gate to generate the final radar image. As an intermediate angular image is computed, it allows an optical view to be processed (according to geometrical considerations).

Therefore, this application provides 4 types of images, such as the bare example of a kind of building as shown in Fig. 4. Anaglyph grants a quick and practical perception of puzzling "3D" scenes.

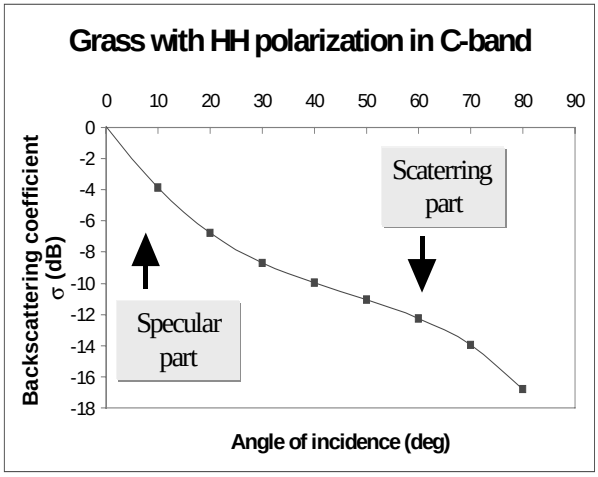

Fig 1: A modelized backscattering coefficient

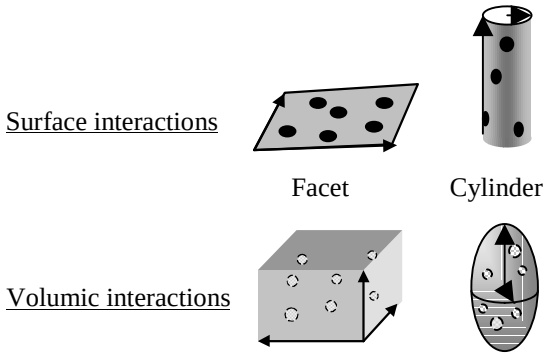

Fig 2: Examples of objects.

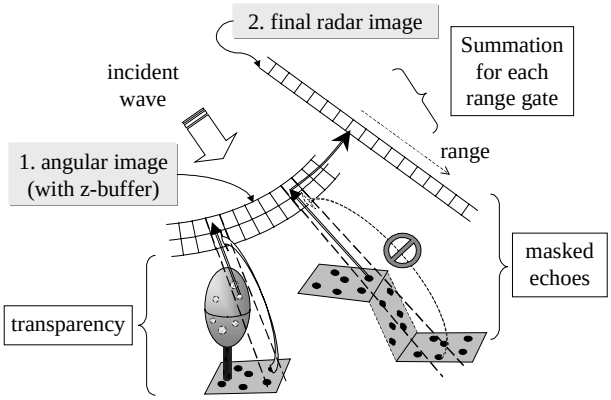

Fig 3: The 2 steps of the image generator.

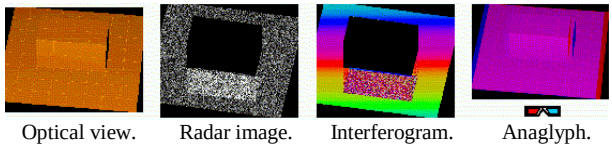

Fig. 4: Types of images produced by 2SIR.

COHERENCE LOSSES

Theoretical Definition

The classical definition of the coherence γ is (3), where x_1 and x_2 are complex images, the function E( ) represents the expectation function; and the operator * is the complex conjugate associated to a complex value.

$$\gamma = \frac{\mathrm{E}\left(x_1.x_2^{*}\right)}{\sqrt{\mathrm{E}\left(x_1.x_1^{*}\right)\mathrm{E}\left(x_2.x_2^{*}\right)}} \qquad (3)$$

This function is often used to characterize the quality of interferograms, however it is a little bit risky to use it. Indeed, in practice, only (4) can be computed. Signals are supposed to be ergodic and locally spatially stationary, thus the expectation function is replaced by a local mean $\langle\ \rangle$.

$$\tilde{\gamma} = \frac{\left\langle x_1.x_2^{*}\right\rangle}{\sqrt{\left\langle x_1.x_1^{*}\right\rangle\left\langle x_2.x_2^{*}\right\rangle}} \qquad (4)$$

Therefore this estimator is maximal when the phase difference is constant, that is, when there are no fringes. Therefore, the more fringes there are, the lower $\tilde{\gamma}$ is. In fact, $\tilde{\gamma}$ evaluates correctly the interferometric noise only if the phase difference is stationary. Besides, the window size (within which the mean operator $\langle\ \rangle$ is computed) affects the quality of the coherence estimator. With small sizes, this estimator is biased [3][7]. With large windows even though the scene is stationary [4][7], $\tilde{\gamma}$ falls off since the phase difference turns if there are fringes (and that is what is expected). Thus the classical coherence as defined in (4) do not well estimate interferograms quality.

Theoretical Effects of Slope and Baseline

Under certain conditions (simultaneous survey or negligible terrain decorrelation and atmospheric effects), the phase difference $\Delta\varphi$ between pixels of the two images correctly coregistered can be approximated by (5). This function depends on geometrical parameters described in Fig. 5, and on the wavelength λ and the coefficient *k* which worths 1 in bistatic case, and 2 in monostatic case.

$$\Delta\varphi = \frac{2\pi}{\lambda}.k.b.\sin\left(\theta-\alpha\right) \qquad (5)$$

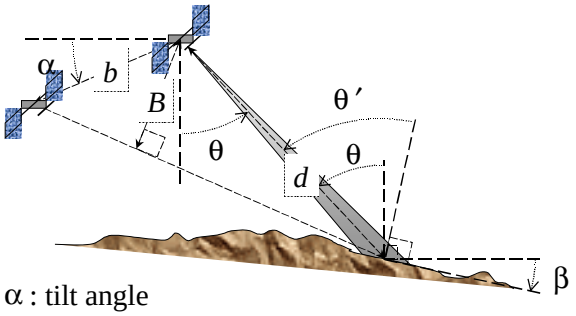

α : tilt angle
b : baseline — β : slope
B : orthogonal baseline — θ : off-nadir angle
d : distance — θ′: incident angle =θ - β

Fig 5: Geometry of acquisitions.

For a little variation of θ, the phase difference $\delta\Delta\varphi$ follows variation of *d* as (6). This formula is equivalent to a frequency shift defined in (7) (where f_0 is the central frequency) [5].

$$\delta\Delta\varphi = -\frac{2\pi}{\lambda}k\frac{b}{d}\frac{\cos\left(\theta-\alpha\right)}{\tan\left(\theta'\right)}\delta d \qquad (6)$$

$$\Delta f = -k.f_0\frac{B}{d.\tan\left(\theta'\right)} \qquad (7)$$

Practical Definition

Coherence becomes a good estimator of interferograms quality if fringes can be subtracted [6]. Nevertheless, those are usually unknown, since this is what we want to study. In (8), a phase function Φ has been introduced to describe fringes that we want to remove [6][7]. Without this knowledge, orbital fringes defined in (9) can at least be deduced, which are fringes due to the baseline on a flat ground. In this case, the slope is null, then θ' equals θ. The coefficient R_d is the slant range resolution, and *n* is the index in range of the pixel. However, if the local slope is known, or a local gradient of fringes can be computed like in (10), it may be subtracted to improve the accuracy of coherence.

$$\tilde{\gamma} = \frac{\left\langle x_1.x_2^{*}.\exp\left(-i\Phi\right)\right\rangle}{\sqrt{\left\langle x_1.x_1^{*}\right\rangle\left\langle x_2.x_2^{*}\right\rangle}} \qquad (8)$$

$$\Phi_{orbital} = -\frac{2\pi}{\lambda}k\frac{b}{d}\frac{\cos\left(\theta-\alpha\right)}{\tan\left(\theta\right)}R_d.n \qquad (9)$$

$$\Phi_{slope} = \left\langle \nabla Phase\left(\frac{x_1 . x_2^{*}}{\sqrt{x_1 . x_1^{*} . x_2 . x_2^{*}}} \right) \right\rangle \qquad (10)$$

APPLICATION

Simulation

The simulations have been defined so that the produced images are representative scenes as we could observe with the ERS system on soil and rock surfaces. In order to compute coherence, one or two facets in the case of layover have been placed according to the geometrical conditions of acquisition. The specific parameters of simulations are fixed in Table 1.

Parameters:	Nominal values
Wavelength λ	0.056 meters
Polarization	VV
Material type	Soil & rock
Slant range resolution R_d	7.9 meters
Azimutal resolution R_a	3.9 meters
Window size in range	4 pixels
Window size in azimut	100 pixels
Mean range of the facet	850 000 meters
Tilt angle α	0 degrees
Local incident angle θ'(for layover only)	23 degrees
Othogonal baseline *B* (for layover only)	250 meters

Table 1: The default values.

In each case, two interferometric radar images are generated, then (8) is computed. The function Φ can be (9) or (10) when the slope is known. Each coherence value is reported in graphs such as in Fig. 6. So as to give the best general survey, each value appears twice, first in a surface representation which gives us an idea of the absolute value, and also in a gray-level image which provides us with an easy way to examine relative variations.

Therefore, in each graph 2×100×100 images are produced. We must notice that when θ' is close to 0 degree or 90 degrees (for a difference lower than approximately 5 degrees), the simulation may be corrupted. The waves, which appear on the edges in Fig. 7 are a good example. This is not a serious weakness because in the cases it happens, the coherence is low.

Simulated Effects of Slope and Baseline

In Fig. 6, we remark the expected coherence losses due to a large baseline and a slope. The Fig. 7 tends to prove that coherence loss is almost due to how coherence is computed. Coherence is much better when the local phase gradient has been previously subtracted, since it is nearly constant and it worths 1. This means that the effect of the phase rotation within pixels is negligible, contrary to the effect of the size of the evaluation window, which is the main cause of coherence loss.

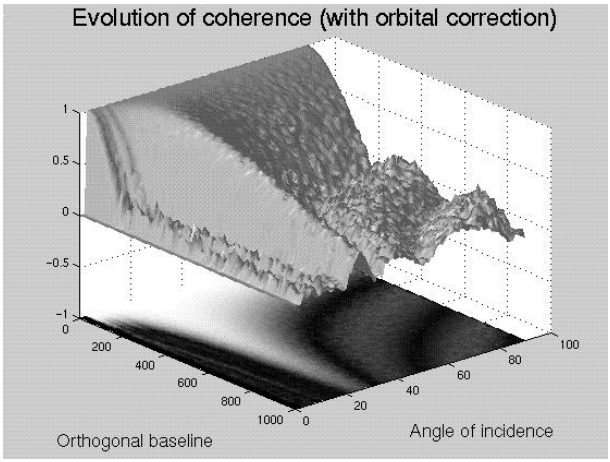

Fig 6: Effects of slope and baseline in the case (9).

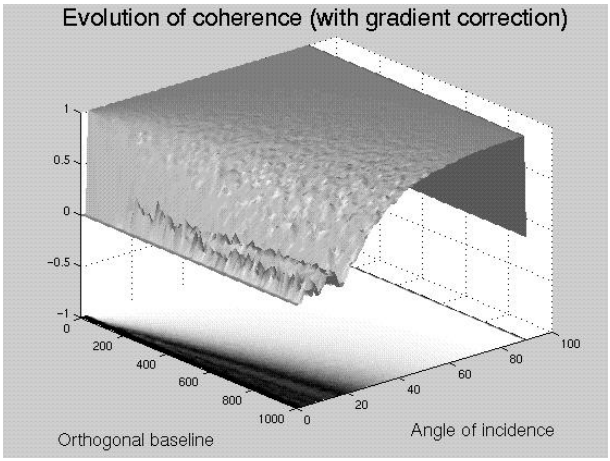

Fig 7: Effects of slope and baseline in the case (10).

Layover

A priori, two types of layover cases can be distinguished. The case of Fig. 8, in which one facet faces the other one, has been named the "positive layover" case. In this occurrence, multi-paths are allowed, and cases of double or triple bounce may be likely, however those phenomena are ignored in this first approach. Moreover, those effects are actually negligible on natural surfaces, which are too rough to admit of coherent effects.

The second case, shown in Fig. 9, can be found on the top of mountains, hills or buildings, and has been called the "negative layover" case. Obviously, it is hardly to be expected that it can be observed without a "positive layover" unless the radar (for example if it is masked)

does not lighten the surface in front of the relief. However, it is interesting to separate the two effects.

The function Φ used in the computation of the coherence is (9). Therefore, Fig. 10 and Fig. 11 show that coherence is even better since each facet is horizontal (*i.e.* there is no residual fringes due to the slope); and because one of them is parallel to the incident wave (*i.e.* little energy is back scattered by the surface, thus only the other one contributes to the signal). On the other hand, coherence is worse when one of the facets is perpendicular to the incident wave. Since the slant range resolution is low, it means that the phase rotation within pixels becomes significant, thus coherence falls off.

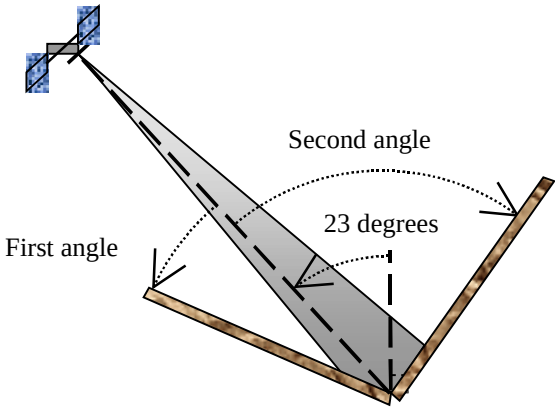

Fig 8: Geometry in the case of the "positive layover".

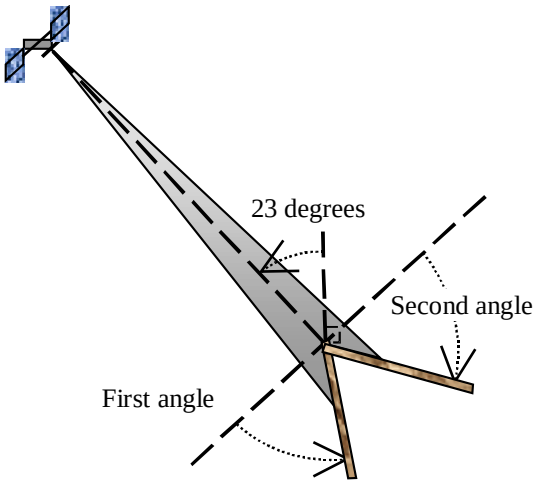

Fig 9: Geometry in the case of the negative layover

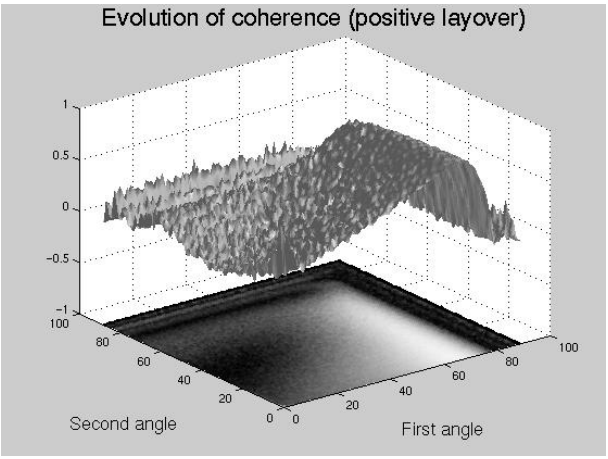

Fig 10: Coherence in the case of the "positive layover".

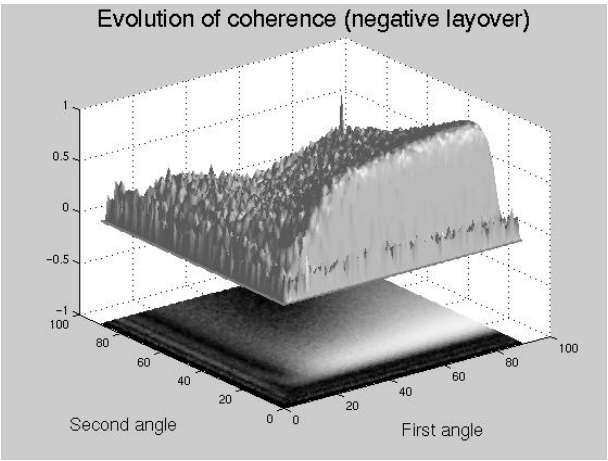

Fig 11: Coherence in the case of "negative layover".

CONCLUSION

Therefore, all the tests done so far (a great number of not yet published tries on fractal relief and other surfaces, has been made) seem to provide realistic simulations. Owing to the great number of parameters available in 2SIR (material, polarization, angles, shape of the objects, …) a perfect validation of the simulator is difficult moreover this is not required for our future studies.

However, the next step will be to make tests on the volumic interactions, then to introduce a management of multiple bounces particularly in urban areas.

ACKNOWLEDGEMENTS

We must express our appreciation to J.D. Durou of the IRIT, L. Neuville and all people who helped us in this task, for giving us their time.

REFERENCES

[1] F. T. Ulaby, M. C. Dobson, “Handbook of radar scattering for terrain”, Artech House editor.

[2] T. F. Bush, F. T. Ulaby, “Fading characteristics of panchromatic radar backscatter from selected agricultural targets”, IEEE Trans. On Geosci. Electronics, vol. GE-13, no 4, pp. 149-157, october 1975.

[3] R. Touzi, A. Lopes, J. Bruniquel, P. Vachon, “Unbiased estimation of the coherence from multi-look SAR data”, IGARSS’ 96, Remote Sensing for a Sustainable Future, Lincoln, Nebraska, IEEE, vol. 1, pp. 662-664.

[4] R. Touzi, “Estimation of stationary and nonstationary coherence in SAR imagery”, IGARSS’ 98, Sensing and Managing the Environment, Seattle, Washington, IEEE proceedings, vol. 5, pp. 2659-2661.

[5] F. Gatelli, A. Monti Guarnieri, F. Parizzi, P. Pasquali, and C. Prati, “The wavenuber shift in SAR Interferometry”, IEEE Transac. on Geosci. and Remote Sensing, vol. 32, no. 4, pp. 855-865, July 1994.

[6] A. Monti Guarnieri, and C. Prati, “SAR interferometry : A ‘quick and dirty’ coherence estimator for data browsing”, IEEE Transac. On Geosci. and Remote Sensing, vol. 35, no. 3, pp. 660-669, May 1997.

[7] R. Touzi, A. Lopes, J. Bruniquel, P.W. Vachon, “Coherence estimation for SAR imagery”, IEEE Transac. On Geosci. and Remote Sensing, vol. 37, no. 1, pp. 135-149, January 1999.

[8] S. Dupont, F. Perlant, M. Berthod, “SAMI: an InSAR simulator to improve SAR calibration”, IGARSS’ 95, Florence, Italy, Quantitative Remote Sensing for Science and Applications, vol. 1, pp. 559-561.

[9] S. N. Madsen, A. Zebker, and J. Martin, “Topographic mapping using radar interferometry : processing techniques”, IEEE Transac. On Geosci. and Remote Sensing, vol. 31, no. 1, pp. 246-256, January 1993.

[10] S. N. Madsen, N. Skou, K. Woelders, and J. Granholm, “EMISAR single pass topographic SAR interferometer modes”, IGARSS’ 96, Remote Sensing for a Sustainable Future, Lincoln, Nebraska, IEEE, vol. 1, pp. 674-676,.

[11] G. Franceschetti, A. Iodice, M. Migliaccio, D. Riccio, “A novel across-track SAR interferometry simulator”, IEEE Transac. On Geosci. and Remote Sensing, vol. 36, no. 3, pp. 950-962, May 98.